BULETINUL ŞTIINŢIFIC

al

Universităţii „POLITEHNICA” din Timişoara, România

Seria AUTOMATICĂ şi CALCULATOARE

SCIENTIFIC BULLETIN

of

The “POLITEHNICA” University of Timişoara, Romania

Transactions on AUTOMATIC CONTROL and COMPUTER SCIENCE

Vol. 57 (71), No. 3, September 2012 Frequency: 4 issues per year
ISSN 1224-600X

EDITURA POLITEHNICA

Scientific Bulletin of The "POLITEHNICA" University of Timişoara, Romania
Transactions on AUTOMATIC CONTROL AND COMPUTER SCIENCE
http://www.ac.upt.ro/journal/
Vol. 57 (71), No. 3, September 2012
ISSN 1224-600X, Frequency: 4 issues per year
Publisher: Editura Politehnica, Bd. Republicii 9, 300159 Timişoara, Romania

Address for editorial correspondence
Prof.dr.ing. Stefan Preitl
"Politehnica" University of Timişoara, Faculty of Automation and Computers, Bd. V. Parvan 2, RO-300223 Timişoara, Romania, Phone: +40-2564032-24, -29, Fax: +40-256403214, E-mail: *stefan.preitl@aut.upt.ro*

http://www.ac.upt.ro/journal/

CONTENTS

BULETINUL ŞTIINŢIFIC al Universităţii „POLITEHNICA" din Timişoara, România,
Seria AUTOMATICĂ ŞI CALCULATOARE
SCIENTIFIC BULLETIN of The "POLITEHNICA" University of Timişoara, Romania,
Transactions on AUTOMATIC CONTROL and COMPUTER SCIENCE, Vol. 57 (71), No. 3, September 2012, ISSN 1224-600X

New Force Functions for the Force Generated by Different Fluidic Muscles

József Sárosi

Technical Institute, University of Szeged, Faculty of Engineering, Mars ter 7, 6724 Szeged, Hungary
Phone: (3662) 546-571, E-Mail: sarosi@mk.u-szeged.hu, http://www.mk.u-szeged.hu/szte_profiles/9

Abstract* — In industrial environment and robotics different types of pneumatic actuators - e. g. cylinders and pneumatic motors - can be found commonly to date. A less well-known type is that of the so-called pneumatic artificial muscles (PAMs). Pneumatic artificial muscle is a membrane that will expand radially and contract axially when inflated, while generating high pulling force along the longitudinal axis. Different designs have been developed, but the McKibben muscle is the most popular and is made commercially available by different companies, e. g. Fluidic Muscle manufactured by Festo Company. There are a lot of advantages of PAMs like the high strength, good power-weight ratio, low price, little maintenance needed, great compliance, compactness, inherent safety and usage in rough environments. The main disadvantage of these muscles is that their dynamic behaviour is highly nonlinear. The layout of this paper is as follows. Section I (Introduction) is a short review of the professional literatures. Section II (Experimental Set-up for Analysis of Fluidic Muscles) is devoted to display our test bed and LabVIEW program. Section III (Static Modelling of Pneumatic Artificial Muscles) describes several force equations and our newest models for the force generated by Fluidic Muscles. Section IV (Experimental Results) compares the measured and theoretical data. Finally, Section V (Conclusion and Future Work) gives the investigations we plan.

***Keywords:* Fluidic Muscle, Static Model, Force Equation, MS Excel Solver.**

I. INTRODUCTION

The working principle of pneumatic artificial muscles is well described in literature ([1], [2], [3], [4], [5] and [6]). Many researchers have investigated the relationship of the force, length and pressure to find a good theoretical approach for the equation of force produced by pneumatic artificial muscles. Some of them report several mathematical models, but significant differences have been noticed between the theoretical and experimental results ([2], [4], [7], [8], [9] and [10]).

Length of artificial muscle depends on force under constant pressure. This force decreases with increasing position of the muscle and the muscle inflates. Our goal is to develop precise approximation algorithms with minimum numbers of parameters for the force of different Fluidic Muscles. Fluidic Muscles type DMSP-20-200N-RM-RM (with inner diameter of 20 mm and initial length of 200 mm) and type DMSP-20-400N-RM-RM (with inner diameter of 20 mm and initial length of 400 mm) produced by Festo Company are selected for this study.

II. EXPERIMENTAL SET-UP FOR ANALYSIS OF FLUIDIC MUSCLES

The experimental set-up (Fig. 1.) consists of a slider mechanism. One side of the muscle is fixed to a load cell, while the other side is attached to the movable frame. The load cell (7923 type from MOM) is a 4 bridge element of strain gauges. It is mounted to the PAM on the fixed surface. The load cell measures the force exerted by the PAM. To measure the air pressure inside the muscle, a Motorola MPX5999D pressure sensor is plumbed into the pneumatic circuit. The linear displacement of the actuator is measured using a LINIMIK MSA 320 type linear incremental encoder with 0.01 mm resolution.

The air pressure applied to the actuator can be regulated with an adjustable regulator (proportional pressure regulator (PPR)) type Festo VPPM-6L-L-1-G1/8-0L6H-V1N-S1C1. The PPR is controlled by voltage inputs. A National Instruments Multi-I/O card (NI 6251) reads the signal of force, pressure sensor and incremental encoder into the PC.

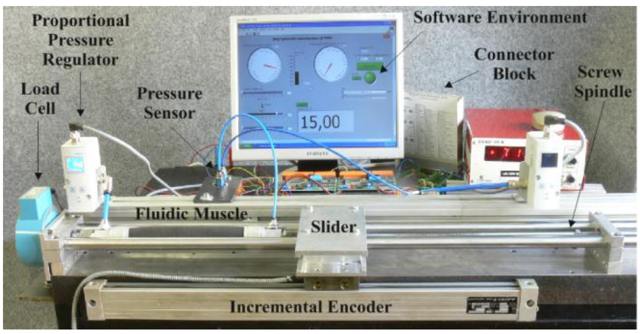

Fig. 1. Experimental set-up for analysis of Fluidic Muscles.

The tests are performed by changing the displacement of the slider. During each test, frame position, muscle force and applied gauge pressure are recorded. With the specially constructed testing machine, we are able to measure the static and dynamic characteristics of several versions of pneumatic actuators.

The software side of this experimental set-up is designed in LabVIEW environment (Fig. 2.). LabVIEW is a typical example for high level software, capable of connecting various kinds of DAQ boards with a PC.

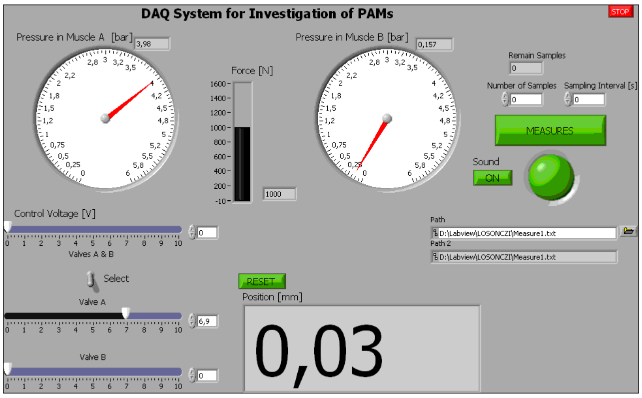

Fig. 2. Front panel of LabVIEW program.

III. Static Modelling of Pneumatic Artificial Muscles

The general behaviour of PAMs with regard to shape, contraction and tensile force when inflated depends on the geometry of the inner elastic part and of the braid at rest (Fig. 3.), and on the materials used [3]. Typical materials used for the membrane construction are latex and silicone rubber, while nylon is normally used in the fibres. Fig. 4. shows the materials of Fluidic Muscles.

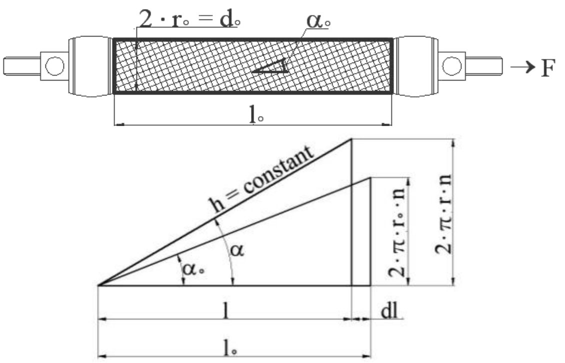

Fig. 3. Geometry parameters of PAMs.

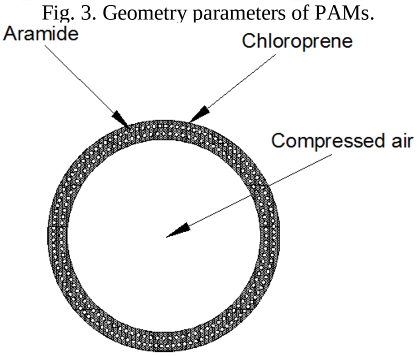

Fig. 4. Materials of Fluidic Muscles.

With the help of [2], [4] and [8], the input and output (virtual) work can be calculated:

$$dW_{in} = p \cdot dV \tag{1}$$

dW_{in} can be divided into a radial and an axial component:

$$dW_{in} = 2 \cdot r \cdot \pi \cdot p \cdot l \cdot (+dr) - r^2 \cdot \pi \cdot p \cdot (\text{-}dl) \tag{2}$$

The output work:

$$dW_{out} = -F \cdot dl \tag{3}$$

By equating the virtual work components:

$$dW_{in} = dW_{out} \tag{4}$$

Using (1) and (3):

$$F = \text{-}p \cdot \frac{dV}{dl} \tag{5}$$

Using (2) and (3):

$$F = \text{-}2 \cdot r \cdot \pi \cdot p \cdot l \cdot \frac{dr}{dl} - r^2 \cdot \pi \cdot p \tag{6}$$

On the basis of Fig. 3.:

$$\cos\alpha_0 = \frac{l_0}{h} \text{ and } \cos\alpha = \frac{l}{h} \tag{7}$$

$$\sin\alpha_0 = \frac{2 \cdot \pi \cdot r_0 \cdot n}{h} \text{ and } \sin\alpha = \frac{2 \cdot \pi \cdot r \cdot n}{h} \tag{8}$$

$$\frac{l}{l_0} = \frac{\cos\alpha}{\cos\alpha_0} \text{ and } \frac{r}{r_0} = \frac{\sin\alpha}{\sin\alpha_0} \tag{9}$$

$$r = r_0 \cdot \frac{\sqrt{1-\cos^2\alpha}}{\sin\alpha_0} = r_0 \cdot \frac{\sqrt{1-\left(\frac{l}{l_0} \cdot \cos\alpha_0\right)^2}}{\sin\alpha_0} \tag{10}$$

$$\frac{dr}{dl} = -\frac{r_0 \cdot l \cdot \cos^2\alpha_0}{l_0^2 \cdot \sin\alpha_0} \cdot \frac{1}{\sqrt{1-\left(\frac{l}{l_0} \cdot \cos\alpha_0\right)^2}} \tag{11}$$

By using (10) and (11) with (6) the force equation is found:

$$F(p,\kappa) = r_0^2 \cdot \pi \cdot p \cdot (a \cdot (1-\kappa)^2 - b) \tag{12}$$

where $a = \frac{3}{tg^2\alpha_0}$, $b = \frac{1}{\sin^2\alpha_0}$, $\kappa = \frac{l_0 - l}{l_0}$, $0 \le \kappa \le \kappa_{max}$,

and *V* the muscle volume, *F* the pulling force, *p* the applied pressure, r_0, l_0, α_0 the initial inner radius and length of the PAM and the initial angle between the thread and the muscle long axis, *r, l, α* the inner radius and length of the PAM and angle between the thread and the muscle long axis when the muscle is contracted, *h* the constant thread length, *n* the number of turns of thread and *κ* the contraction.

Consequently:

$$F_{max} = r_0^2 \cdot \pi \cdot p \cdot (a - b), \text{if } \kappa = 0 \quad (13)$$

and

$$\kappa_{max} = 1 - \sqrt{\frac{b}{a}}, \text{if } F = 0 \quad (14)$$

Equation (12) is based on the admittance of a continuously cylindrical-shaped muscle. The fact is that the shape of the muscle is not cylindrical on the end, but rather is flattened, accordingly, the more the muscle contracts, the more its active part decreases, so the actual maximum contraction ration is smaller than expected [4].

Tondu and Lopez in [4] consider improving (12) with a correction factor ε, because it predicts for various pressures the same maximal contraction. This new equation is relatively good for higher pressure ($p \geq 200$ kPa). Kerscher, Albiez, Zöllner and Dillmann in [8] suggest achieving similar approximation for smaller pressure another correction factor μ is needed, so the modified equation is:

$$F(p,\kappa) = \mu \cdot r_0^2 \cdot \pi \cdot p \cdot (a \cdot (1 - \varepsilon \cdot \kappa)^2 - b) \quad (15)$$

where $\varepsilon = a_\varepsilon \cdot e^{-p} - b_\varepsilon$ and $\mu = a_\kappa \cdot e^{-\kappa \cdot 40} - b_\kappa$.

Significant differences between the theoretical and experimental results using (12) and (15) have been shown in [11] and [12]. To eliminate the differences new approximation algorithms with six and five unknown parameters have been introduced for the force generated by Fluidic Muscles:

$$F(p,\kappa) = (a \cdot p + b) \cdot e^{c \cdot \kappa} + d \cdot p \cdot \kappa + e \cdot p + f \quad (16)$$

$$F(p,\kappa) = (p + a) \cdot e^{b \cdot \kappa} + c \cdot p \cdot \kappa + d \cdot p + e \quad (17)$$

Equation (16) can be generally used with high accuracy for different Fluidic Muscle independently from length and diameter under different values of pressure and (17) can be used with high accuracy for Fluidic Muscle with inner diameter of 20 mm, only.

The unknown parameters of (16) (a, b, c, d, e and f) and (17) (a, b, c, d and e) can be found by Solver in MS Excel 2010.

IV. EXPERIMENTAL RESULTS

Our analyses were carried out in MS Excel environment. Tensile force of Fluidic Muscles under different values of constant pressure is a function of muscle length (contraction) and air pressure. The force always drops from its highest value at full muscle length to zero at full inflation and position. (Fig. 5. and Fig. 6.).

Firstly, the measured data and force model using (16) were compared. The unknown parameters of (16) were found using Solver in MS Excel. Values of these unknown parameters are shown in Table 1. and Table 2.

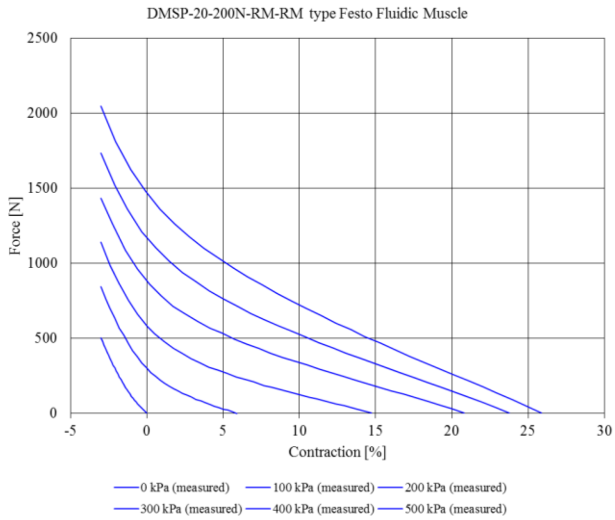

Fig. 5. Isobaric force-contraction diagram of Fluidic Muscle (with DMSP-20-200N-RM-RM).

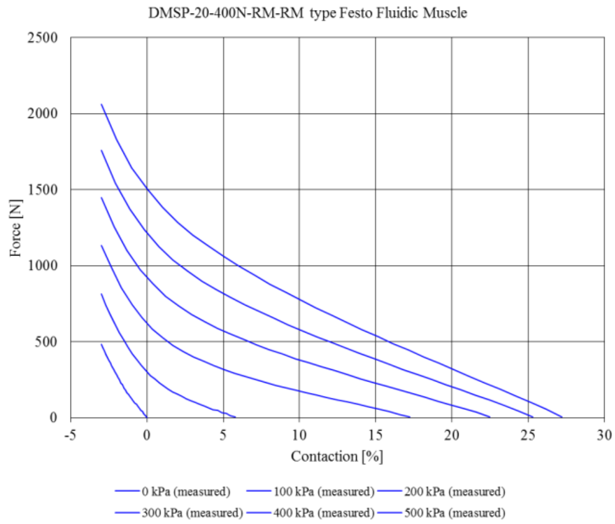

Fig. 6. Isobaric force-contraction diagram of Fluidic Muscle (with DMSP-20-400N-RM-RM).

TABLE 1. Values of unknown parameters (for DMSP-20-200N-RM-RM).

Parameters	Values
a	-4.00180705
b	292.4620246
c	-0.32930845
d	-9.33564098
e	294.0538256
f	-280.498151

TABLE 2. Values of unknown parameters (for DMSP-20-400N-RM-RM).

Parameters	Values
a	-4.35572689
b	281.2237983
c	-0.32866293
d	-9.27034945
e	302.2010663
f	-263.691854

The accurate fitting of (16) can be seen in Fig. 7. and Fig. 8.

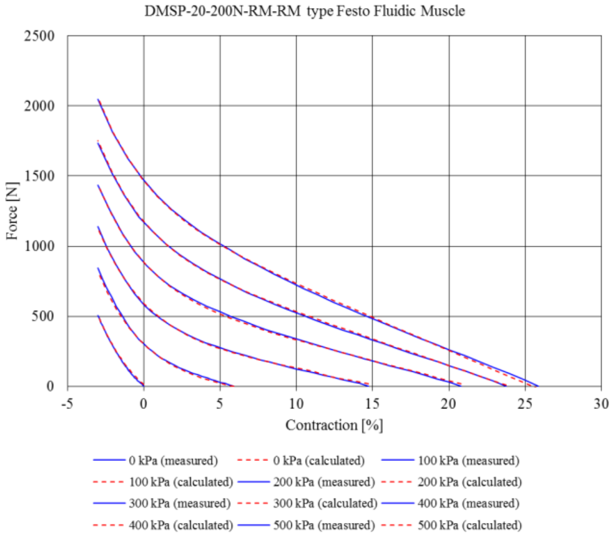

Fig. 7. Comparison of measured data and force model using (16) (with DMSP-20-200N-RM-RM).

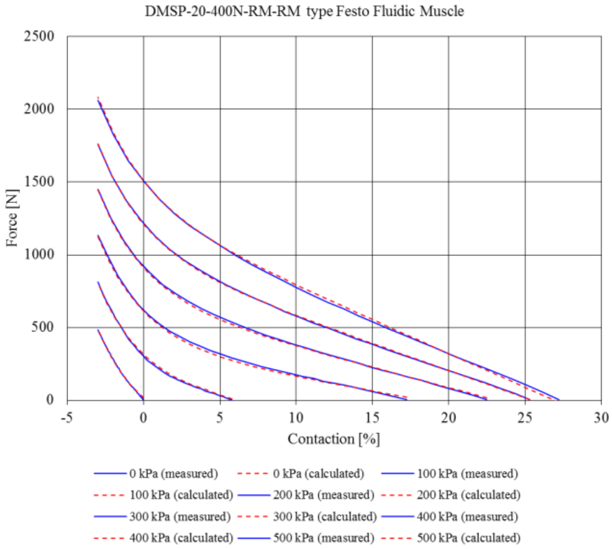

Fig. 8. Comparison of measured data and force model using (16) (with DMSP-20-400N-RM-RM).

Fig. 9. and Fig. 10. illustrate the relationship between the measured force and calculated force. The R^2 = 0.9995 → R = 0.9997 correlation index proves the tight relationship between them.

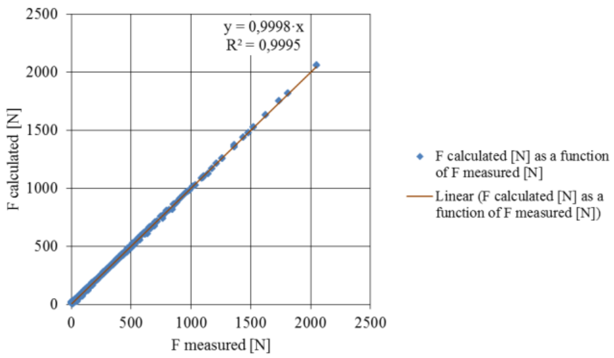

Fig. 9. Relationship between the measured force and calculated force using (16) (with DMSP-20-200N-RM-RM).

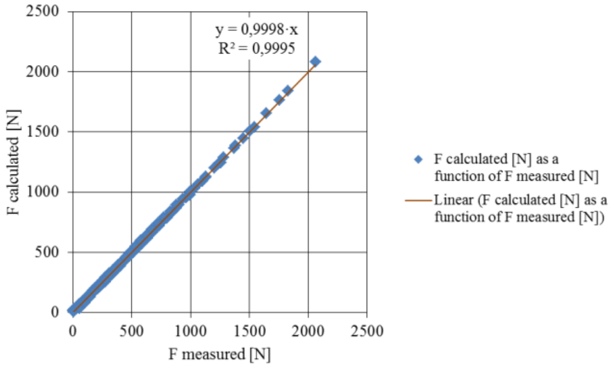

Fig. 10. Relationship between the measured force and calculated force using (16) (with DMSP-20-400N-RM-RM).

Secondly, the investigations using (17) were repeated. Values of unknown parameters of (17) are listed in Table 3. and Table 4.

TABLE 3. Values of unknown parameters (for DMSP-20-200N-RM-RM).

Parameters	Values
a	286.1714546
b	-0.327523456
c	-9.135794264
d	288.4720479
e	-271.3462159

TABLE 4. Values of unknown parameters (for DMSP-20-400N-RM-RM).

Parameters	Values
a	274.7944784
b	-0.32623809
c	-9.07369264
d	296.3161465
e	-254.042387

The results of (17) and measured data can be compared in Fig. 11. and Fig. 12. In Fig. 13. and Fig. 14. are shown the accurate approximation of the measured force (R^2 = 0.9994 → R = 0.9997 correlation index and R^2 = 0.9993 → R = 0.9996 correlation index).

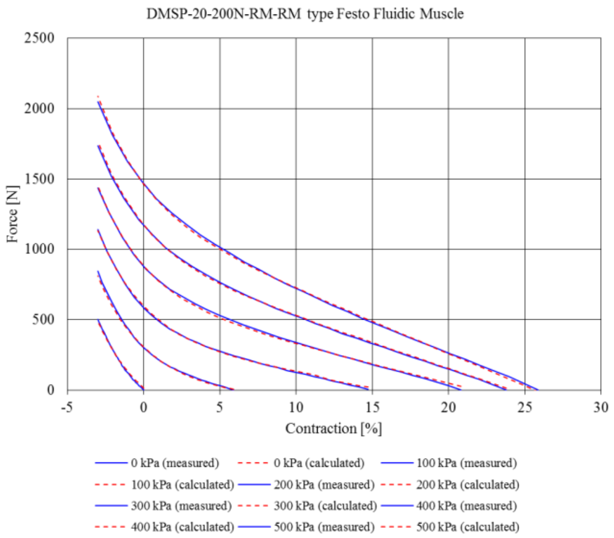

Fig. 11. Comparison of measured data and force model using (17) (with DMSP-20-200N-RM-RM).

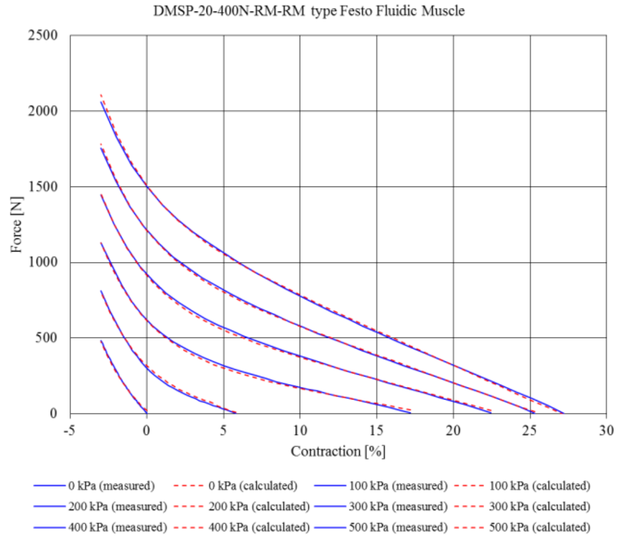

Fig. 12. Comparison of measured data and force model using (17) (with DMSP-20-400N-RM-RM).

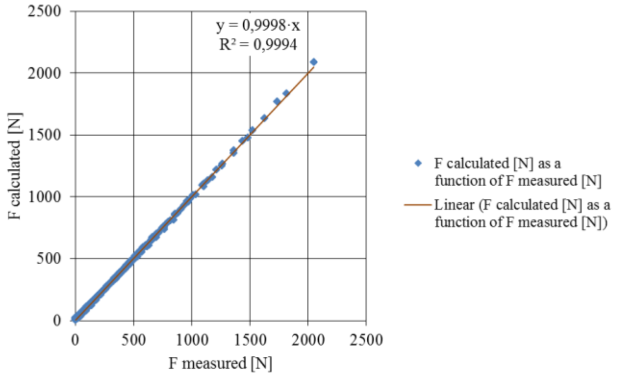

Fig. 13. Relationship between the measured force and calculated force using (17) (with DMSP-20-200N-RM-RM).

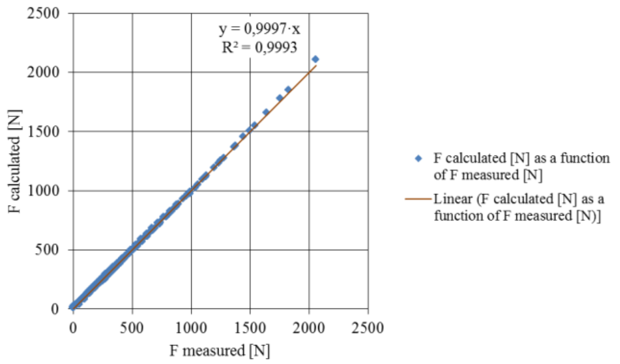

Fig. 14. Relationship between the measured force and calcula.ted force using (17) (with DMSP-20-400N-RM-RM).

The precise positioning of PAMs requires accurate determination of the dynamic model of pneumatic actuators. Therefore the hysteresis in the tension-length (contraction) cycle of PAMs was analysed.

Chou and Hannaford in [2] report hysteresis to be substantially due to the friction, which is caused by the contact between the bladder and the shell, between the braided threads and each other, and the shape changing of the bladder. Some experiments were made to illustrate the hysteresis (Fig. 15. and Fig. 16.).

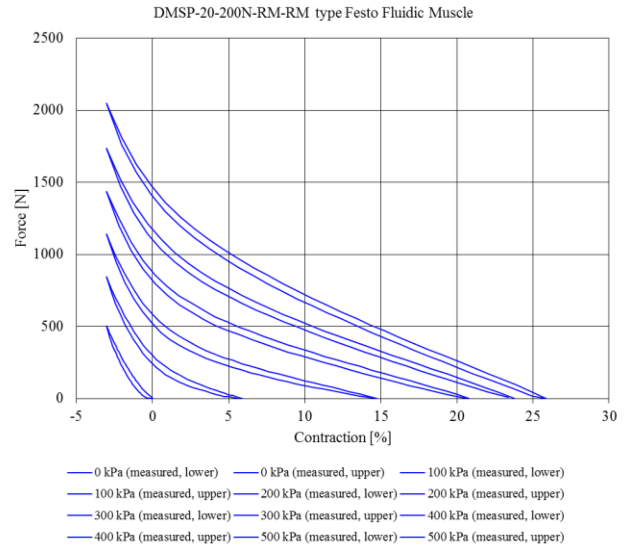

Fig. 15. Hysteresis in the tension-length (contraction) cycle (with DMSP-20-200N-RM-RM).

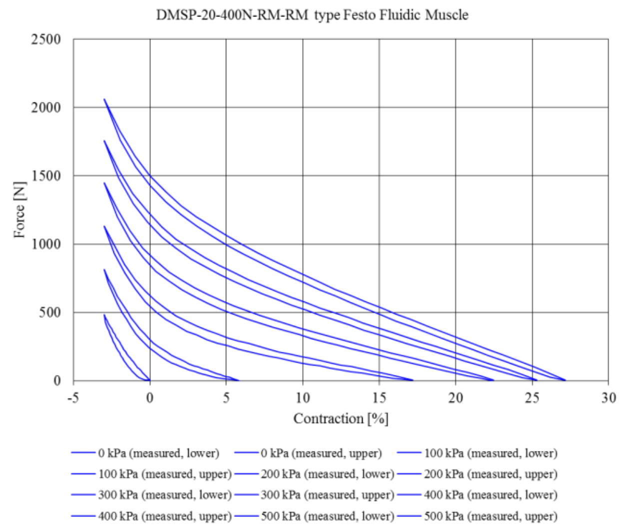

Fig. 16. Hysteresis in the tension-length (contraction) cycle (with DMSP-20-400N-RM-RM).

To approximate the hysteresis loop using (17), besides the parameters in Table 3. and Table 4., new parameters had to be specified (Table 5. and Table 6.).

TABLE 5. Values of unknown parameters (for DMSP-20-200N-RM-RM).

Parameters	Values
a	253.938042
b	-0.3712419
c	-9.1342021
d	285.066068
e	-293.91895

TABLE 6. Values of unknown parameters (for DMSP-20-400N-RM-RM).

Parameters	Values
a	235.183308
b	-0.3803548
c	-9.0612216
d	293.793153
e	-282.57012

Approximation of hysteresis loop using (17) can be seen in Fig. 17. and Fig. 18.

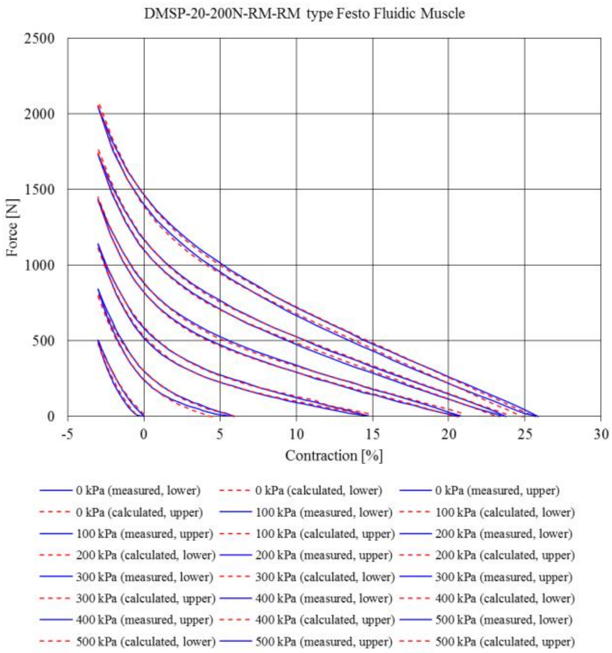

Fig. 17. Approximation of hysteresis loop using (17) (with DMSP-20-200N-RM-RM).

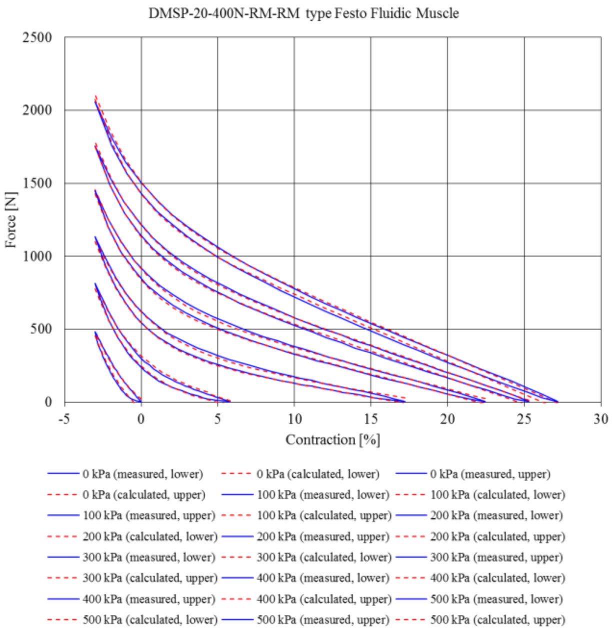

Fig. 18. Approximation of hysteresis loop using (17) (with DMSP-20-400N-RM-RM).

V. Conclusions

In this work new accurate functions for the force produced by different Festo Fluidic Muscles have been introduced. The accuracy of fittings has been proved with comparisons of the measured and theoretical data. Our aim is to develop a new general mathematical model for pneumatic artificial muscles on the basis of our new models.

References

[1] D. G. Caldwell, A. Razak and M. J. Goodwin, “Braided Pneumatic Muscle Actuators”, Proceedings of the IFAC Conference on Intelligent Autonomous Vehicles, Southampton, UK, 1993, pp. 507-512.

[2] C. P. Chou and B. Hannaford, “Measurement and Modeling of McKibben Pneumatic Artificial Muscles”, IEEE Transactions on Robotics and Automation, vol. 12, no. 1, pp. 90-102, 1996/

[3] F. Daerden, “Conception and Realization of Pleated Artificial Muscles and Their Use as Compliant Actuation Elements”, PhD Dissertation, Vrije Universiteit Brussel, Faculteit Toegepaste Wetenschappen Vakgroep Werktuigkunde, Bruxelles, Belgium, 1999, pp. 5-33.

[4] B. Tondu and P. Lopez, “Modeling and Control of McKibben Artificial Muscle Robot Actuators”, IEEE Control Systems Magazine, vol. 20, no. 2, pp. 15-38, 2000.

[5] F. Daerden and D. Lefeber, “Pneumatic Artificial Muscles: Actuator for Robotics and Automation”, European Journal of Mechanical and Environmental Engineering, vol. 47, pp. 10-21, 2002.

[6] M. Balara and A. Petík, “The Properties of the Actuators with Pneumatic Artificial Muscles”, Journal of Cybernetics and Informatics, vol. 4, pp. 1-15, 2004.

[7] N. Yee and G. Coghill, “Modelling of a Novel Rotary Pneumatic Muscle”, Proceedings of Australiasian Conference on Robotics and Automation, Auckland, New Zealand, 2002, pp. 186-190.

[8] T. Kerscher, J. Albiez, J. M. Zöllner and R. Dillmann, “FLUMUT - Dynamic Modelling of Fluidic Muscles Using Quick-Release”, Proceedings of 3rd International Symposium on Adaptive Motion in Animals and Machines, Ilmenau, Germany, 2005, pp. 1-6.

[9] R. Ramasamy, M. R. Juhari, M. R. Mamat, S. Yaacob, N. F. Mohd Nasir and M. Sugisaka, “An Application of Finite Element Modeling to Pneumatic Artificial Muscle”, American Journal of Applied Sciences, vol. 2, no. 11, pp. 1504-1508, 2005.

[10] J. Borzikova, M. Balara and J. Pitel, “The Mathematical Model of Contraction Characteristic k = (F, p) of the Pneumatic Artificial Muscle”, Proceedings of XXXII. Seminar ASR '2007 “Instruments and Control”, Farana, Smutný, Kočí & Babiuch, Ostrava, Czech Republic, 2007, pp. 21-25.

[11] J. Sárosi and Z. Fabulya: “New Function Approximation for the Force Generated by Fluidic Muscle”, International Journal of Engineering, Annals of Faculty of Engineering Hunedoara, vol. 10, no. 2, pp. 105-110, 2012.

[12] J. Sárosi, Z. Fabulya, G. Szabó and P. Szendrő: ”Investigations of Precise Function Approximation for the Force of Fluidic Muscle in MS Excel”, Review of Faculty of Engineering (International Conference on Science and Technique in the Agri-Food Business, ICoSTAF 2012), vol. 2012/3-4, pp. 1-8, 2012.

Manuscript received June 26, 2012; revised September 22, 2012; accepted for publication September 27, 2012.